Elimination of the Non-Axisymmetric inter-ELM Heat Flux Generated by Resonant Magnetic Perturbations in High Density Divertor Conditions

A.R. Briesemeister[1], J.W. Ahn[1], J.M. Canik[1], M.E. Fenstermacher[2], H. Frerichs[3], C. J. Lasnier[2], J.D. Lore[1], A.W. Leonard[4], M.A. Makowski[2], A.G. McLean[2], W.H. Meyer[2], O. Schmitz[3], M.W. Shafer[1], E.A. Unterberg[1], J. G. Watkins[5]

[1]Oak Ridge National Laboratory, Oak Ridge, TN, USA
[2]Lawrence Livermore National Laboratory, Livermore, CA, USA
[3]University of Wisconsin-Madison, Madison, WI, USA
[4]General Atomics, San Diego, CA, USA
[5]Sandia National Laboratories, Albuquerque, NM, USA

E-mail contact of main author: briesemeister@fusion.gat.com

Keywords: detachment

Abstract. It is found that asymmetries in heat flux arising from resonant field perturbations are eliminated as density is raised to approach detached divertor conditions on DIII-D. It is shown that applying RMPs reduces the core density and increases the inter-ELM peak heat flux to both the inner and outer targets in the divertor. Using gas puffing to return the core density to the pre-RMP levels reduces the inter-ELM heat flux at the outer strike point to a value just below the pre-RMP level; the heat flux profile is broadened slightly relative to the pre-RMP profile. It is also shown that further increasing the plasma density eliminates the non-axisymmetric heat flux broadening, even before the attainment of detached conditions. Both experimental evidence and modeling are presented showing that neither detachment nor the elimination of the 3D field structure is needed to eliminate the non-axisymmetric heat flux broadening. Measurements showing that a secondary peak in the ion saturation current, observed at modest densities, is not present at high densities. Measurements are presented showing that in cases where the application of RMPs leads to an increase in the core electron temperature, higher densities are needed to induce detachment of the outer strike point. These results help alleviate concerns over potential heat and particle load asymmetries that may arise with the use of 3D ELM control techniques, and are particularly encouraging for future reactors where near detached conditions will be required in any case to reduce divertor heat and particle loads.

1. Background

Scaling studies for ITER and future devices generally show that tools will be needed to reduce or eliminate both the steady state heat flux and the transient heat flux from ELMs. RMPs have been shown to effectively suppress, mitigate or trigger ELMs on several devices [1][2][3][4]. RMPs are therefore being considered as a tool to control ELMs in ITER [5]. However, RMPs also lead to localized hot spots on plasma facing components of the divertor, and thus concerns remain about the compatibility of the steady state heat flux footprint with the divertor structure [6].

Detachment has been shown to be an important tool to control steady state heat and particle flux to the divertor. Concerns about the compatibility of detachment and RMPs have been raised because of results showing that increasing density can increase heat flux to regions further from the strike [7,8]. Although the heat flux to these regions is generally lower than the peak heat flux in attached conditions, and therefore this spreading of the heat flux can be beneficial, modeling shows that in ITER RMPs may increase the heat flux to more vulnerable, highly shaped, regions of the divertor [6]. Additionally at DIII-D it has been observed that higher levels of gas puffing are needed to detach the inner strike point when RMPs are applied [9] and at NSTX it has been observed that adding RMPs can cause a detached divertor to re-attach [10].

Additionally, it has been observed that the RMP induced non-axisymmetries can appear in the particle flux structure while the heat flux structure remains axisymmetric. At low densities particle flux profiles in DIII-D have shown splitting while the heat flux profile remains relatively unperturbed by RMPs [11]. At higher densities in DIII-D, and at NSTX, the particle and heat flux profiles have similar structure [8][12]. Simulations have shown that changes in fueling may be responsible for the differences between the heat and the particle flux structure, [13] reinforcing the need to better understand the relationship between heat and particle flux structures and their relationships to density and fueling.

Since changes in core conditions will generally affect divertor conditions [14] it is important to understand how RMP induced changes in the core conditions will impact divertor conditions. A reduction in core density, known as pumpout, typically occurs when RMPs are applied to low collisionality plasmas. At DIII-D pumpout has been observed in low collisionality plasmas, but is not typically seen in high collisionality plasmas even in cases with ELM suppression [8]. No pumpout in high collisionality ELM mitigated discharges was observed in ASDEX Upgrade [15], but RMP induced pumpout was seen at low density [15].

2. Using Fueling to Eliminate Pumpout Induced Increase in Heat Flux

It is shown in this section that applying RMPs can increase the peak heat flux between ELMs to the divertor in cases with core density pumpout, but this increase is largely eliminated when the core density is raised to the pre-RMP level. *FIG. 1.(a)* shows that when RMPs are applied the core density as a fraction of Greenwald density [16] is reduced from n_e/n_{GW} =0.37 to n_e/n_{GW} =0.26. Electron density here is the line averaged density measured by the interferometer, [17] and $n_{GW}=I_p/\pi a^2$ where I_p is the total plasma current and a is the average minor radius of the plasma. For all the data used in this paper RMPs were generated using the upper and lower I-coils in an n=3 even parity configuration.

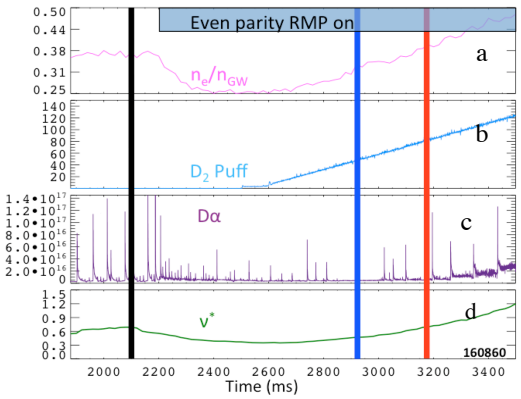

FIG. 1. The (a) line averaged electron density as a fraction of Greenwald density, (b) gas puffing rate, (c) Deuterium emission line strength and (d) pedestal electron collisionality are shown as a function of time. Vertical lines indicated the time slices chosen for detailed analysis.

The reduction in core density is eliminated when deuterium is added by gas puffing at the crown of the plasma. Gas puffing is initiated 300 ms after the RMPs are applied and increased until the core density equals and then exceeds the pre-RMP level. In this discharge after the RMPs were applied the ELM size was reduced by the application of the RMPs. This change can be seen in the deuterium Balmer-α line signal measured in the divertor by the filterscopes [18] and shown in *FIG.1.(c)*. The reduction in deuterium emission was correlated with a reduction in the energy released by the ELMs measured by the fast magnetics.

The electron collisionality is measured at the top of the pedestal, and drops to a minimum value of ν_e=0.35. The reduction in ELM size and a temporary gap in ELMs shortly after 2.8 s are consistent with the typical onset of ELM suppression [11]. Collisionalities below ν_e=0.3 are typically needed for robust ELM

suppression with even parity RMPs [4], but were not achieved in this experiment.

The discharges shown throughout this paper had an edge safety factor of q_{95}=3.5 which is within the range where low-collisionality ELM suppression has been achieved in DIII-D. A typical lower single null shape was used with the ion $B \times \nabla B$ drift direction towards the divertor. The toroidal field was B_t =1.9 T and neutral beam heating of 6 MW was used. In this section a shape with moderate lower triangularity, which puts the outer strike point near the inlet of the cryopump, was chosen to maximize pumpout. Data in subsequent sections was collected in a shape with reduced lower triangularity to allow better diagnostic measurements of the outer strike point.

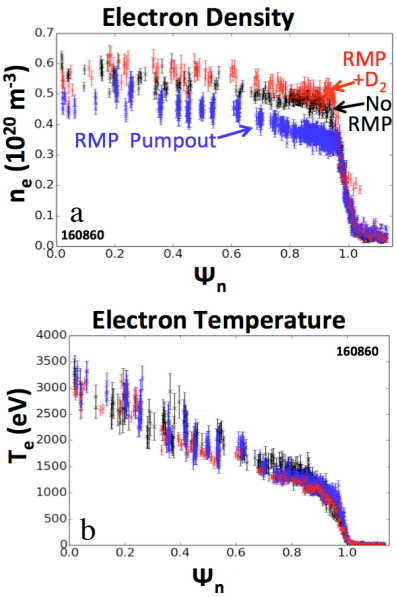

FIG. 2. The electron (a) density and (b) temperature profiles are shown for the three time slices indicated in Fig. 1.

Three time-slices from the discharge, indicated by vertical lines on *FIG. 1.*, were chosen for detailed analysis. Data at 2.1 s was chosen to represent pre-RMP plasma conditions. The second slice at 2.9 s was chosen to be in the middle of the ELM-free time window. At 3.2 s the core density was found to match the pre-RMP density.

At time slices where the line-averaged densities are similar the core electron density and temperature profiles are similar regardless of whether RMPs are applied. In *FIG. 2.(a)* it can be seen that the densities are similar in the pre-RMP time slice and the case in which gas puffing has been used to raise the plasma density across the entire profile. During the RMP induced density pumpout the density profile from the SOL to the top of the pedestal is nearly identical to that seen in the other two time slices. The pedestal height in the case with density pumpout is reduced by just over 25%. The density gradients inside the pedestal region are similar to those in the other two cases. *FIG. 2.(b)* shows neither the RMPs nor the added gas had a measurable effect on the electron temperature.

Heat flux to the divertor is measured by the IRTV system [19,20]. Integration times of 62 μs are used. Each profile shown in *FIG. 3.* is the average of multiple frames captured during a 200 ms interval. In intervals with ELMs, only frames captured during the last 20% of the ELM cycle were used.

As shown in *FIG. 3.(a)* before the RMPs are applied there is no measurable heat flux to the inner strike point. During the RMP induced pumpout the heat flux to the inner strike point is increased, but adding deuterium eliminates the heat flux to the inner strike point. This indicates that the reduction in core density is largely responsible for the increase in heat flux.

The outer strike point shows a similar trend, but as is typical for discharges with the field direction configured so that the $B \times \nabla B$ drift is directed towards the divertor, the peak heat flux to the outer target was much larger than the heat flux to the inner strike point. As shown in *FIG. 3.(b),* applying the RMPs raises the peak heat flux to the outer strike point. When the core density with RMP is matched to the pre-RMP level the peak heat flux is slightly reduced, and the heat flux profile is broadened by the presence of the RMPs. These measurements show that RMPs can reduce the inter-ELM heat flux at the outer strike point when compared to cases with comparable core densities. Heat flux measured at the outer strike point at a

single toroidal location has been found to be largely axisymmetric both in modelling and in experiments, such as those presented in section 3, where the RMPs were moved relative to the heat flux diagnostic. Away from the outer strike point larger toroidal variations may exist in the heat flux.

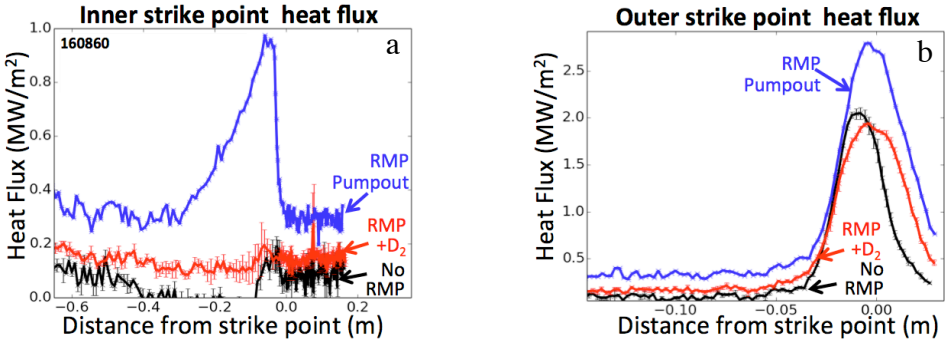

FIG. 3. The heat flux between ELMs to the (a) inner and (b) outer strike points are shown for the three time slices indicated in FIG.1.

The magnetic configuration used for the measurements shown in this section limits the outboard radial extent of heat flux seen by the IRTV camera due to shadowing from the divertor shelf, which limits analysis of the heat flux outboard of the outer strike point. This configuration was chosen because it is the configuration in which low collisionality ELM suppression is typically achieved (due to proximity to a cryopump that aids low collisionality access) and in which maximum RMP induced pumpout is observed. The next section features data from a configuration with more extensive divertor diagnostic coverage.

3. Increasing Density can Eliminate Non-axisymmetric Structure in Heat and Particle Flux

Since heat flux profile measurements are currently only available at a single toroidal location, the non-axisymmetric structure is measured by moving the applied RMP field relative to the diagnostics. By reversing the current in all the coils used to create the RMP fields, the magnetic structures can be effectively shifted 60 degrees toroidally around the machine. *FIG. 4.* shows heat flux measurements with the coils in both the 0 and 60 degree configuration. Although the lobe structures are not well separated in this discharge the effects of the RMPs on the heat flux structure can be seen in the lower density case, with a core density of n_e/n_{GW} =0.4, shown in *FIG.4.(a)*. When the coils are moved from a 0 degree phasing to a 60 degree phasing local changes of up to 0.4 MW/m^2 can be seen in the heat flux profile, indicating non-axisymmetric structure. *FIG.4.(b)* shows that at higher density, n_e/n_{GW} =0.75, the heat flux to the tiles is reduced and shows no measurable non-axisymmetric structure is seen.

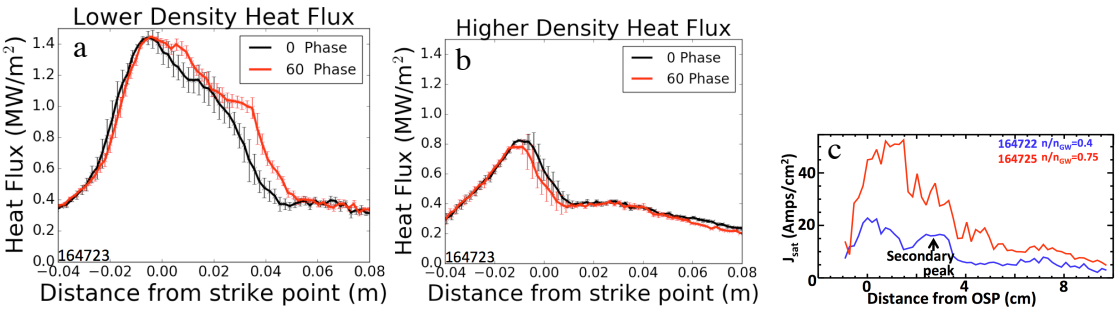

FIG. 4. The heat flux profile near the outer strike point is shown for a (a) moderate upstream density and (b) high upstream density. (c) The ion saturation current measured at the target near the outer strike point is shown for a lower density (blue) and higher density (red) case with RMPs.

Simulations have shown that increased divertor density can reduce the non-axisymmetric heat flux while raising the particle flux to the striations [13]. The Langmuir probes in the divertor target tiles [21] are used to measure the particle flux. To increase the spatial resolution of these measurements the plasma is swept radially relative to the probe area and the data is re-mapped to a single equilibrium. In *FIG. 4.(c)* the re-mapped profiles for both the low and high-density cases are shown. A secondary peak can be seen in the lower density case, but at higher densities there is no apparent secondary peak.

3.1. Changes Seen in Divertor Electron Temperature and Density

The divertor Thomson scattering system measures changes in the electron temperature consistent with lobe structures induced by the RMPs. As shown in *FIG. 5.,* when RMPs are applied a lobe in the electron temperature appears to extend from the x-point outwards towards a point on the target about 10 cm outboard of the outer strike point. No such structure appears in the case without RMPs [22]. The temperature in this lobe is about 10 eV above the plasma that surrounds it. The plasmas shown in *FIG. 5.(a) and (b)* are attached with an upstream density of Greenwald density is n/nGW=0.4. Although some structure is seen in the electron density when the RMPs are applied it is much less pronounced than the structure seen in the electron temperature.

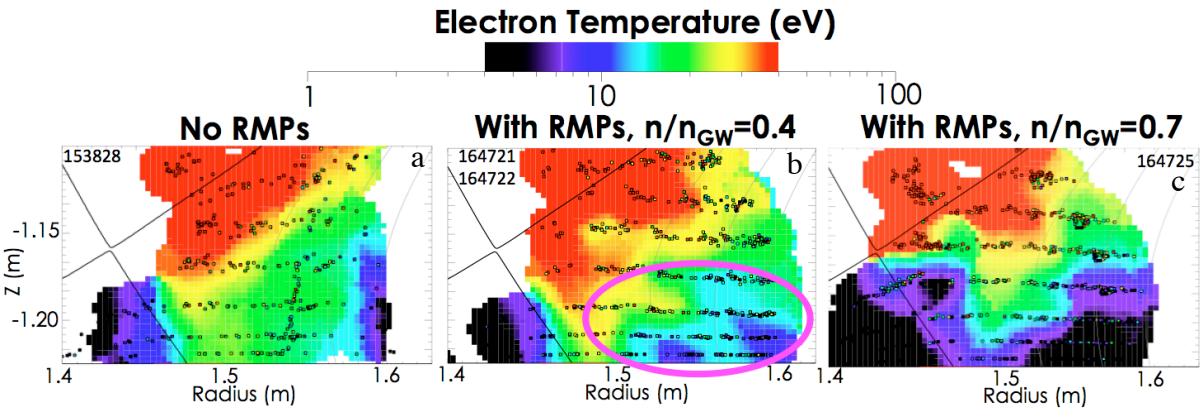

FIG. 5. The electron temperature in the divertor is shown a) without RMPs, b) with RMPs at a lower density and c) with RMPs at a higher density.

As the density is increased, the lobes in the electron temperature move away from the target plate. As shown in *FIG. 5.(c),* although structure remains in the electron temperature, there is no longer a clear secondary peak at the target. The electron density also shows no secondary peak at the target. At this higher density the divertor is not yet detached.

4. Comparisons of Measurements with EMC3-Eirene Modeling

The EMC3-Eirene 3D edge fluid modeling code [23,24] shows that when upstream density is increased while all other quantities are held fixed, the experimentally observed changes in the divertor electron temperature are reproduced. In the lower density calculations shown in *FIG. 6.(a)* the lobes in the electron temperature in the divertor extend to the target plate. As the density at the upstream simulation boundary is increased the lobes in the electron temperature, shown in *FIG. 6.(b),* are preferentially cooled near the target plate. This change in structure is qualitatively similar to that shown in FIG. 5.

In these simulations the magnetic field structure and perpendicular transport coefficients are held constant while the density at the core simulation boundary, chosen to be at the normalized enclosed flux surface Ψ_n=0.7, was varied. A "vacuum" model for the 3D magnetic field structure is used – this does not include plasma response fields to RMPs. Since the plasma response can change with density, the "vacuum" field was chosen to test the effects of increasing core density in the absence of changes in the magnetic field structure.

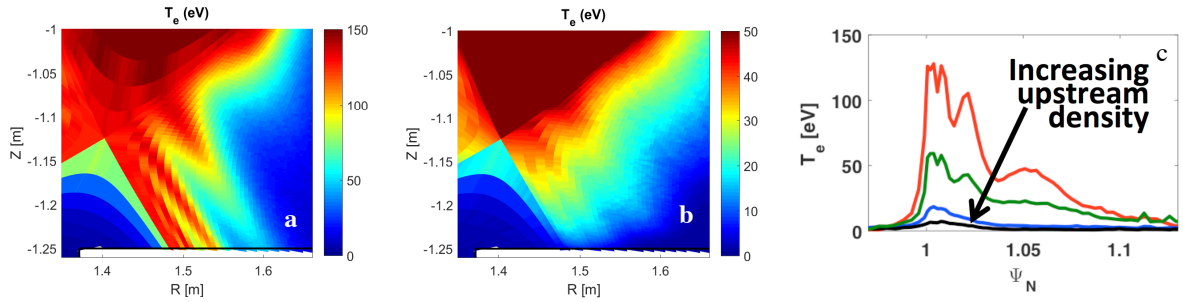

FIG. 6. The electron temperature in the divertor calculated for (a) lower and (b) higher upstream density conditions. (c) The electron temperature at the target plate calculated by the EMC3-Eirene code is shown for a variety of upstream densities.

Examining the calculated electron temperature at the target plate, shown in *FIG.6.*, it can be seen that increasing the core density causes a reduction in both the temperature at the outer strike point and a reduction in the local peaks away from the outer strike point. The electron temperature peak at the outer strike point is largely axisymmetric, showing less than a 10% variation toroidally. The secondary peaks show much larger toroidal variations in the lower density calculations, but these peaks are gradually eliminated at all toroidal angles as the upstream density is increased.

5. RMPs Increase the Detachment Onset Threshold

Examining two high-density cases shows evidence that RMPs raise the detachment onset threshold for the outer strike point. *FIG. 7.* shows the ion saturation current profiles measured by Langmuir probes near the outer strike point for two relatively high-density plasmas. The case without RMPs shows a strong reduction in the saturation current at the outer strike point and the peak in the saturation current is moved radially outboard. This structure is characteristic of detachment at the strike point. The profile with RMPs shows a peak in the saturation current near the outer-strike point. This profile is characteristic of the outer strike point being in the high-recycling regime.

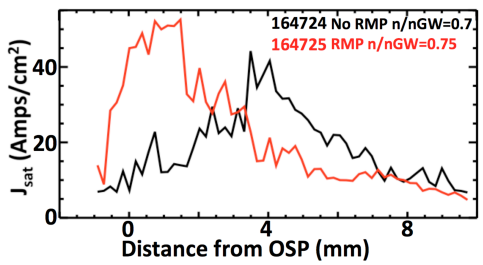

FIG. 7. The saturation current at the floor shows that the divertor plasma is in the high-recycling regime with RMPs (red), but detached at a slightly lower upstream density without RMPs (black).

A slight reduction in the core temperature possibly caused by the presence of a rotating MHD mode in the case with no RMPs may be responsible for the differences in detachment between the cases with and without RMPs. The electron temperature is 10 to 20 percent higher across

the core profile in the case with RMPs. In the case with no RMPs a rotating mode with a toroidal number of 2 is present for the steady state portion of the discharge. In the discharge with RMPs this mode only appears after the RMPs are turned off. This dramatic modification of the MHD modes by the RMPs was not observed in the other discharges presented in this work and appears to be correlated with the high densities used in this set of discharges.

The differences in the level of divertor detachment between the cases with and without RMPs cannot be explained by differences in core density. The line-averaged density in the case without RMPs is found to be 8.1×10^{19} m^{-3} while in the case with RMPs it is 8.3×10^{19} m^{-3}. Notable, just inside the separatrix at Ψ_n=0.99 the density is 20 percent higher in the case with RMPs and there is no measurable difference in the density at the separatrix with and without RMPs. Other parameters such as plasma current, magnetic field strength and auxiliary heat power were held fixed between the two cases.

6. Conclusion

It has been shown that while the relationship between core and divertor conditions are largely similar to what is observed in axisymmetric plasmas some notable modifications are observed when RMPs are applied. In cases where RMPs cause density pumpout, but no measureable change in the core electron temperature, the associated increase in heat flux is largely eliminated by raising the core density. When the application of RMPs causes an increase in core electron temperature an increase in the divertor detachment threshold as a function of density is seen. RMPs can cause measurable broadening of the inter-ELM heat flux at moderate densities, but this broadening is eliminated at high densities. Lobes in the electron temperature structure are induced by the RMPs and extend to the floor at moderate densities, but at high densities these structures move away from the floor. The cooling of these structures is consistent with cooling seen in the simulations in which the core density is raised. Modeling shows that the electron temperature near the target plate becomes largely axisymmetric as the density is raised, consistent with the measurements which show the heat flux becomes axisymmetric at high densities.

This work is suported by the U.S. Department of Energy under DE-AC04-00OR22725[1], DE-AC52-07NA27344[2], DE-FG02-08ER54999[3], DE-F02-04ER54698[4] and DE-AC04-94AL85000[5]. DIII-D data shown in this paper can be obtained by following the links at https:// fusion.gat.com/global/D3D_DMP.

7. References

[1] SUTTROP, W. et al., First Observation of Edge Localized Modes Mitigation with Resonant and Nonresonant Magnetic Perturbations in ASDEX Upgrade, Phys. Rev. Lett. **106** 22 (2011) 225004.
[2] CANIK, J.M. et al., On Demand Triggering of Edge Localized Instabilities Using External Nonaxisymmetric Magnetic Perturbations in Toroidal Plasmas, Phys. Rev. Lett. **104** 4 (2010) 45001.
[3] CANIK, J.M. et al., ELM destabilization by externally applied non-axisymmetric magnetic perturbations in NSTX, Nucl. Fusion **50** 3 (2010) 34012.
[4] KIRK, A. et al., Understanding the effect resonant magnetic perturbations have on ELMs, Plasma Phys. Control. Fusion **55** 12 (2013) 124003.
[5] LANG, P.T. et al., ELM control strategies and tools: status and potential for ITER, Nucl. Fusion **53** 4 (2013) 43004.
[6] SCHMITZ, O. et al., Three-dimensional modeling of plasma edge transport and divertor fluxes during application of resonant magnetic perturbations on ITER, Nucl. Fusion **56** 6 (2016) 66008.

[7] AHN, J.-W. et al., Characterization of divertor footprints and the pedestal plasmas in the presence of applied n = 3 fields for the attached and detached conditions in NSTX, Plasma Phys. Control. Fusion **56** 1 (2014) 15005.
[8] JAKUBOWSKI, M.W. et al., Overview of the results on divertor heat loads in RMP controlled H-mode plasmas on DIII-D, Nucl. Fusion **49** 9 (2009) 95013.
[9] PETRIE, T.W. et al., Results from radiating divertor experiments with RMP ELM suppression and mitigation, Nucl. Fusion **51** 7 (2011) 73003.
[10] AHN, J.-W. et al., Effect of nonaxisymmetric magnetic perturbations on divertor heat and particle flux profiles in National Spherical Torus Experiment, Phys. Plasmas 1994 **18** 5 (2011) 56108.
[11] SCHMITZ, O. et al., Aspects of three dimensional transport for ELM control experiments in ITER-similar shape plasmas at low collisionality in DIII-D, Plasma Phys. Control. Fusion **50** 12 (2008) 124029.
[12] AHN, J.-W., et al., Modification of divertor heat and particle flux profiles with applied 3D fields in NSTX H-mode plasmas, Nucl. Fusion **50** 4 (2010) 45010.
[13] FRERICHS, H., et al., Striation pattern of target particle and heat fluxes in three dimensional simulations for DIII-D, Phys. Plasmas 1994-Present **21** 2 (2014) 20702.
[14] STANGEBY, P.C., The Plasma Boundary of Magnetic Fusion Devices, Institute of Physics Pub., Bristol; Philadelphia (2000).
[15] SUTTROP, W. et al., Studies of edge localized mode mitigation with new active in-vessel saddle coils in ASDEX Upgrade, Plasma Phys. Control. Fusion **53** 12 (2011) 124014.
[16] GREENWALD, M., Density limits in toroidal plasmas, Plasma Phys. Control. Fusion **44** 8 (2002) R27.
[17] ZEELAND, M.A.V., et al., Fiber optic two-color vibration compensated interferometer for plasma density measurements, Rev. Sci. Instrum. **77** 10 (2006) 10F325.
[18] COLCHIN, R.J., et al., The Filterscope, Rev. Sci. Instrum. **74** 3 (2003) 2068.
[19] HILL, D.N. et al., Infrared thermography of the DIII□D divertor targets, Rev. Sci. Instrum. **59** 8 (1988) 1878.
[20] LASNIER, C.J. et al., Survey of target plate heat flux in diverted DIII-D tokamak discharges, Nucl. Fusion **38** 8 (1998) 1225.
[21] WATKINS, et al., High heat flux Langmuir probe array for the DIII-D divertor platesa), Rev. Sci. Instrum. **79** 10 (2008) 10F125.
[22] MCLEAN, A.G. et al., Electron pressure balance in the SOL through the transition to detachment, J. Nucl. Mater. **463** (2015) 533.
[23] FENG, Y., et al., A 3D Monte Carlo code for plasma transport in island divertors, J. Nucl. Mater. **241** (1997) 930.
[24] FENG, Y., et al., 3D fluid modelling of the edge plasma by means of a Monte Carlo technique, J. Nucl. Mater. **266–269** (1999) 812.